

Experimental evaluation of shearing effects in volume holograms formed in bleached photographic emulsions

A. Beléndez

Departamento de Ingeniería de Sistemas y Comunicaciones
Universidad de Alicante
Apdo. nº 99. Alicante E 03080 (SPAIN)

L. Carretero and A. Fimia

Laboratorio de Optica
Departamento Interuniversitario de Optica
Universidad de Alicante
Apdo. nº 99. Alicante E 03080 (SPAIN)

Phone: 34 - 6 - 590 35 09 FAX: 34 - 6 - 590 34 64

Short title: Evaluation of shearing effects in bleached volume holograms

ABSTRACT

Transmission holograms recorded in Agfa 8E75 HD photographic emulsion and processed with an R-9 reversal bleach are analyzed experimentally. Several important aspects related to the influence of recording materials and their processing on the design of holographic optical elements have been considered. The case of the two plane wave as well as that of the spherical object wave are analyzed in detail. Emphasis is on the estimation of shear angles from their effects on hologram properties. The influence of exposure, spatial frequency and slant angle on shear angles is briefly analyzed and discussed.

KEY WORDS: Bleached holograms, Thickness and index changes, Shearing effects

1.- Introduction

Holographic optical elements (HOE's) are currently incorporated into several optical systems. For some applications, such as head-up displays¹ or optical interconnects², the HOE's have proven superior to conventional optical elements. However, unlike conventional elements, the design methods for HOE's have not yet been standardized. The holographic recording material and its processing play an important role in the field of design because in order to design an HOE it is necessary to consider not only the change in wavelength between recording and reconstruction, but also the variations in the medium due to processing. Usually these HOE's are recorded as volume phase holograms, and bleached photographic emulsion is an important medium for making volume phase HOE's. This is due to its relatively high sensitivity, improved processing chemistries, the ease of processing of this material, and the repeatability of the results.

Since the publication of Vilkomerson and Bostwick's paper³ on the effects of emulsion shrinkage on a hologram's image space, many studies on the influence of the recording material and its processing on HOE properties have been published⁴⁻⁷. In the chemical processing of silver halide holograms we use liquid solutions. As a consequence, there is a change in the average refractive index and a deformation of the recording material. Due to the compensation of elastic forces during processing, there is a deformation of the volume material and a change in the Bragg planes' orientation. As a result of these variations, the grating vectors before and after processing are different.

It is possible to consider three effects related to processing: variations in the average refractive index, changes in thickness and shear-type effects⁵. Due to these effects, there is a problem associated with the making of a volume HOE: the reconstruction geometry corresponding to maximum diffraction efficiency has to be changed with respect to the obtention geometry, which evidently gives rise to the appearance of aberrations in the HOE during the reconstruction stage⁸⁻¹⁰. Therefore, when we want to design an HOE it is necessary to thoroughly analyze the holographic recording material and the processing that we are going to use, and in order to analyze a recording material -such as bleached photographic emulsions- for

the fabrication of an HOE, we must consider several holographic parameters such as diffraction efficiency, angular and spectral sensitivities, signal-to-noise ratio, environmental stability, refractive index variations, emulsion thickness changes and shear-type effects.

The shear effect is due to the inclination itself of the Bragg planes and therefore this effect must be function of the slant angle of Bragg planes. This lateral motion can be explained by considering the lateral shearing forces that turn the Bragg planes or by considering the tendency of the medium to moving laterally owing to the planes themselves⁵.

In this paper we consider and analyze experimentally the shear-type effects (characterized by the shear angle) caused by chemical processing for transmission gratings and lenses recorded in bleached photographic emulsions, considering firstly other holographic parameters such as the variation in the average refractive index and changes in emulsion thickness.

2.- Variation in the Bragg angle as a function of the changes in the recording material

During processing of a photographic emulsion the physical properties of the material undergo a substantial change. The mechanism that causes those changes is far from clear, but we can measure their effects on hologram properties⁵⁻⁷. Variations in the average refractive index and thickness, and the shearing effects of the holographic recording material that are introduced by the chemical process in a HOE, produce a reordering of the internal structure of the interference fringes. It is this clear to see that the processed and recording elements are different. Several researchers have suggested models for analyzing these effects. Of these models, we will consider the Effective Holographic Grating Model (EHGM)⁵ which works under the assumption that interference fringes before and after processing are planes.

In order to analyze the influence of the average refractive index and thickness and the shear angles on the deviation of the Bragg angle, let us consider a holographic grating recorded in the air by two plane waves. The geometric structure of the holographic grating before and after processing is shown in Figure 1. Average signal and reference beams O and R are incident on

the photographic emulsion at angles θ_O and θ_R , respectively. Inside the emulsion of refractive index n_R these angles are θ'_O and θ'_R . The bisector of the beams inside the emulsion represents a fringe set with period Λ and slant angle ϕ , as measured from the direction normal to the recording material. It is possible to obtain ϕ as follows:

$$\tan \phi = \frac{\cos \theta'_R - \cos \theta'_O}{\sin \theta'_R - \sin \theta'_O} \quad \text{or} \quad \phi = -\frac{1}{2} (\theta'_R + \theta'_O) \quad (1)$$

Let Δt_R define the amount of shrinkage or swelling so that:

$$t_C = t_R + \Delta t_R = t_R \left(1 + \frac{\Delta t_R}{t_R}\right) \quad (2)$$

where t_C is the new thickness of the emulsion and t_R is the original thickness. n_C is the average refractive index after processing and we define Δn_R as:

$$n_C = n_R + \Delta n_R = n_R \left(1 + \frac{\Delta n_R}{n_R}\right) \quad (3)$$

In Figure 1, t_e is the effective thickness of the holographic grating and is related to the real thickness t_C as follows⁵:

$$t_e = \frac{\tan \phi}{\tan \delta + \tan \phi} t_C \quad (4)$$

where δ is the shear angle, similar to those described in the theory of elasticity, and it takes into account the lateral shift of the emulsion ($t_R \cdot \tan \delta$). The shear effect is due to the inclination of the Bragg planes, and angle δ is a function of angle ϕ . The effective thickness includes two deformation effects: the emulsion thickness change and the shearing effect. This parameter appears when we consider a homogeneous deformation of the recording material due to processing⁵. From equation (4) we deduce that for symmetrical gratings ($\phi = 0^\circ$), δ will equal 0° , and for reflection gratings ($\phi \sim 90^\circ$), $t_e \approx t_C$, so that for these gratings the shear effects are not

important. On the other hand, these shear-type effects are more important for small slant angles.

t_C and δ appear in equation (4). While the value of t_C can be easily determined through experimentation, the direct measurement of δ is obviously quite complicated. In order to relate this shear angle to parameters characteristic of the grating, we can refer to Figure 2, which shows the change in Bragg plane OP due to processing when considering the emulsion thickness change and the shearing effect. For the point P of the medium before processing we consider that the shearing (change in form but not in volume) transforms this point into another point P_1 , and the thickness change transforms point P_1 into P^* . The following relationship can be obtained from this figure:

$$t_R \cdot \tan \delta = t_C \cdot \tan \phi^* - t_R \cdot \tan \phi \quad (5)$$

This expression relates the angle of Bragg plane inclination before (OP) and after processing (OP*), ϕ and ϕ^* , respectively, and the thicknesses before and after processing (t_R and t_C), with the shear angle, δ . From Figure 2 it is easy to see that:

$$t_R \cdot \tan \phi = t_e \cdot \tan \phi^* \quad (6)$$

where $t_e = ON$ is the effective thickness. By using equations (5) and (6) it is easy to derive equation (4). On the other hand, t_e relates the Cartesian components of the grating vector before, \mathbf{K} , and after processing, \mathbf{K}^* , as follows⁵:

$$K_x^* = K_x \quad \text{and} \quad K_z^* = \frac{t_R}{t_e} K_z \quad (7)$$

If we assume that the reading angle θ_C is equal to the writing angle θ_R , the efficiency of the diffracted beam by the processed hologram is not maximum; however that diffracted beam propagates in the same direction as the original signal beam; i.e., $\theta_I = \theta_O$, because the surface spacing of the grating before and after processing is unchanged⁷. If this spacing were changed,

the grating would be destroyed⁵. The efficiency of the diffracted beam can reach the maximum by changing the reading angle θ_C by the quantity of $\Delta\theta_B$. In this case θ_C is the Bragg angle after processing and $\Delta\theta_B$ is the deviation in the Bragg angle required for maximum diffraction efficiency reconstruction. It is clear that if $\Delta\theta_B = \theta_C - \theta_R$, then we can write:

$$\theta_C = \theta_R + \Delta\theta_B \quad (8)$$

In Figure 1, $\Delta\theta_B < 0$. It is possible to determine the effective thickness t_e through experimentation by measuring the reconstruction angle θ_C that complies with Bragg's law using the equation⁵:

$$t_e = \frac{n_C}{n_R} \frac{\sin \theta_R + \sin \theta_O}{2 \sin \theta_C + \sin \theta_O - \sin \theta_R} t_R \quad (9)$$

In this equation we have supposed that the reconstruction wavelength, λ_C , is equal to the recording wavelength, λ_R .

By using equations (2), (3), (4), (8) and (9) it is possible to obtain the deviation in Bragg angle $\Delta\theta_B$ as a function of the refractive index variation, Δn_R , the emulsion thickness change, Δt_R , and the shear angle, δ , as follows:

$$\Delta\theta_B \approx \frac{\sin \theta_R + \sin \theta_O}{2 \cos \theta_R \tan \phi} \left[\delta + \left(\frac{\Delta n_R}{n_R} - \frac{\Delta t_R}{t_R} \right) (\delta + \tan \phi) \right] \quad (10)$$

In order to obtain equation (10) we have taken into account that usually $\Delta n_R \ll n_R$, $\Delta t_R \ll t_R$, and $\Delta\theta_B$ and δ are small angles. Based on this we have made the following approximations:

$$\sin \theta_C = \sin (\theta_R + \Delta\theta_B) \approx \sin \theta_R + \Delta\theta_B \cos \theta_R \quad (11)$$

$$\tan \delta \approx \delta \quad (12)$$

and

$$\frac{t_R n_C}{t_C n_R} - 1 = \left(1 + \frac{\Delta n_R}{n_R}\right) \left(1 + \frac{\Delta t_R}{t_R}\right)^{-1} - 1 \approx \frac{\Delta n_R}{n_R} - \frac{\Delta t_R}{t_R} \quad (13)$$

On the other hand, if the deviation of the Bragg angle, $\Delta\theta_B$, and the changes in thickness, Δt_R , and index, Δn_R , are known, it is possible to evaluate the shearing effects experimentally through the obtention of the shear angle δ by using the following equation:

$$\delta \approx \frac{2 \cos \theta_R \tan \phi}{\sin \theta_R + \sin \theta_O} \left[1 - \left(\frac{\Delta n_R}{n_R} - \frac{\Delta t_R}{t_R} \right) \right] \Delta\theta_B - \left(\frac{\Delta n_R}{n_R} - \frac{\Delta t_R}{t_R} \right) \tan \phi \quad (14)$$

This means, in turn, that the shear angle (and the lateral shift of the emulsion, $t_R \cdot \tan \delta$) can be found by measuring the angle of deviation of the Bragg angle and the changes in thickness and refractive index of the emulsion.

3.- Two plane studies

The two plane wave holographic structure is useful in the study of the fundamental characteristics of recording materials, e.g., the sensitivity, diffraction efficiency and signal-to-noise ratio. In our experiments the interference pattern of two plane waves coming from a He-Ne laser ($\lambda_R = 632.8$ nm) is recorded inside the Agfa 8E75 HD photographic emulsion. Each grating with a specific shear angle was recorded on a separate plate. These plates have a nominal 6- μ m thick emulsion and the refractive index of the preprocessed emulsion is $n_R = 1.64$ at a 632.8 nm wavelength¹¹. The exposed plates were developed in AAC developer made up of ascorbic acid and sodium carbonate. The developed plates were rinsed briefly and bleached without a fixation step¹² with R-9, a reversal bleach, which consists of a diluted acidified solution of potassium dichromate. R-9 bleach produces a dissolution and removal of the developed silver, leaving a phase hologram made up of the unexposed silver halide grains. R-9 bleach acts brusquely owing to its solvent action and this produces considerable thickness and

index variations. The processing procedure and the developer and bleach bath formulae are given in Tables I and II.

After processing, the holographic gratings are replayed with a plane wave coming from the same He-Ne laser ($\lambda_C = 632.8$ nm). The diffracted beam intensity is measured and the diffraction efficiency is calculated as the ratio between the power in the first diffracted order and the incident power less the calculated losses due to reflection at the surfaces of the plates.

3.1.- Measurement of index and thickness changes

Initial experiments were aimed at characterizing the material after exposure and processing. This required determination of the refractive index, n_C , and the thickness, t_C , of the emulsion layer. Syms and Solymar¹³ used an interferential method to estimate the thickness, by measuring the modulation produced in the light transmitted by an emulsion with a spectrometer. Other authors¹⁴ have proposed other methods for measuring the index and thickness for photographic emulsions. However we determined both parameters, index and thickness changes, as a function of exposure by analyzing the shift in the most efficient wavelength when we reconstructed holographic reflection gratings at two angular orientations and with different replay wavelengths. A set of reflection gratings were recorded with two collimated beams illuminating the plates from opposite sides. The two beams were incident on the plate normally and 632.8 nm radiation was used with exposures between 30 and 700 $\mu\text{J}/\text{cm}^2$. For this recording geometry the interference fringes are parallel to the hologram surface, the grating vector is perpendicular to the hologram surface and the slant angle is $\phi = 90^\circ$. Taking this into account, and using equation (4), we obtain that t_e is equal to t_C . The exposed plates are processed with an AAC developer and an R-9 bleach bath. At replay, we illuminated the processed grating with a plane wave incident normal to the plate (replay angle θ_C equal to 0°) and at angle $\theta_C = 35^\circ$. We also vary the reconstruction wavelength to obtain minimum intensity in the transmitted beam (maximum intensity in the first diffracted order). If λ_C and λ'_C are the reconstruction

wavelengths for maximum efficiency when the reconstruction angles are $\theta_C = 0^\circ$ and $\theta'_C = 35^\circ$, respectively, by using Bragg's law it is easy to obtain the following equation for $\theta_C = 0^\circ$:

$$\frac{t_C n_C}{t_R n_R} = \frac{\lambda_C}{\lambda_R} \quad (15)$$

and for $\theta'_C = 35^\circ$:

$$\frac{t_C}{t_R n_R} (n_C^2 - \sin^2 \theta'_C)^{1/2} = \frac{\lambda'_C}{\lambda_R} \quad (16)$$

From equations (15) and (16) we can obtain the average refractive index and the thickness, n_C and t_C , respectively, as follows:

$$n_C = \frac{\sin \theta'_C}{[1 - (\lambda'_C/\lambda_C)^2]^{1/2}} \quad (17)$$

and:

$$t_C = \frac{\lambda_C n_R t_R}{\lambda_R n_C} \quad (18)$$

The absolute errors of θ and λ are 0.5° and 0.2 nm, respectively, and the errors in n_C and t_C are 0.01 and 0.06 μm , respectively.

In order to experimentally obtain an empirical relation between the index and thickness changes and the exposure, we plotted the values of $(\Delta n_R/n_R) - (\Delta t_R/t_R)$ obtained from the values of n_R and t_R , and n_C and t_C , as a function of exposure as we can see in Figure 3. In this figure solid curve shows the adjustment of the experimental data when using a cubic polynomial curve and a least squares method. For exposures between 30 and 670 $\mu\text{J}/\text{cm}^2$ we obtained the empirical function:

$$\frac{\Delta n_R}{n_R} - \frac{\Delta t_R}{t_R} = a_0 + a_1 E + a_2 E^2 + a_3 E^3 \quad (19a)$$

where E is the incident exposure and is expressed in $\mu\text{J}/\text{cm}^2$ and the coefficients are:

$$a_0 = 2.630 \times 10^{-2} \quad (19b)$$

$$a_1 = 5.478 \times 10^{-4} \text{ cm}^2/\mu\text{J} \quad (19c)$$

$$a_2 = -1.886 \times 10^{-6} \text{ cm}^4/(\mu\text{J})^2 \quad (19d)$$

$$a_3 = 1.552 \times 10^{-9} \text{ cm}^6/(\mu\text{J})^3 \quad (19e)$$

Equations (19) will be used in the following sections to estimate the values of the shear angle for holographic gratings and lenses.

3.2.- Measurement of the shear angles

In order to analyze the shear-type effects in photographic emulsions bleached with an R-9 bleach bath, transmission gratings were formed with two plane waves having the same intensity and beam size (their diameters were ~ 2 cm). Gratings were recorded with different exposures and with interbeam angles ($|\theta_R| + |\theta_O|$) of 40° and 50° in air. Different recording geometries and the values corresponding to slant angles and spatial frequencies are given in Table III. As we can see in this table, spatial frequency shows almost no change for a fixed interbeam angle. The processed holographic gratings were replayed with a collimated beam of ~ 1 cm diameter at different angles of incidence, θ_C . We rotated the holographic plate and measured the diffracted power at each position. We obtained the reconstruction angle that provided maximum diffraction efficiency. This allowed us to obtain the deviation of the Bragg angle, $\Delta\theta_B$. In all cases we analyzed, a displacement of the replay angle for maximum efficiency with respect to the angle of the reference beam is observed.

In Figure 4 we have plotted the change $\Delta\theta_B$ in the angle of incidence of the read-out wave for the maximum value of the diffracted wave from that of the reference wave (see equation (8)), as a function of exposure for different values of the slant angle and for interbeam angles of (a) 50° and (b) 40° . As we can see from Figure 4, for an interbeam angle of 50° there is a significant value for $\Delta\theta_B$ in the exposure region around the $200 \mu\text{J}/\text{cm}^2$ value. We have not found a reason

that justifies these anomalous values of $\Delta\theta_B$ which appear for all slant angles when the interbeam angle is 50° .

If the deviation in the Bragg angle, $\Delta\theta_B$, is known and we use equation (19) to estimate the values of $(\Delta n_R/n_R) - (\Delta t_R/t_R)$, it is possible to obtain the shear angles δ by using equation (14). The values of the calculated shear angles are plotted in Figure 5 as a function of exposure for the different values of the slant angle of the transmission gratings. The absolute errors for the shear angles vary between 0.1° and 0.4° . The lower values for the errors correspond to the lower values of the slant angle. To obtain these errors we have taken into account that the absolute errors in Δt_R , Δn_R and $\Delta\theta_B$ were $0.1 \mu\text{m}$, 0.02 and 0.1° , respectively. As we can see from Figure 5, shear angles are higher for an interbeam angle of 50° ($\delta \leq 8^\circ$) than for an interbeam angle of 40° ($\delta \leq 1.5^\circ$). From Figure 5 we can draw two important conclusions. Firstly, for a particular recording material, processing and recording geometry, the shear angle is a function of the exposure used during recording and a function of the spatial frequency f because the values obtained for δ are different for interbeam angles of 40° and 50° (different spatial frequencies). By analyzing Figure 5 we can conclude that shear angles are different for different spatial frequencies when the slant angle is fixed. And secondly, as the shear effect is due to the inclination itself of the Bragg planes, then the shear angle must be a function of the slant angle. From Figure 4 the influence of ϕ on δ is clear.

For an interbeam angle of 50° there is a significant anomalous increase in the shear angle value for an exposure of $\sim 200 \mu\text{J}/\text{cm}^2$, although we do not know why. In Figure 6 we have plotted the shear angle δ as a function of exposure for an interbeam angle of 50° and for a slant angle of 13.92° . In this figure the dotted line links the experimental points and the solid line corresponds to the theoretical adjustment of the experimental data without taking into account the anomalous point for an exposure of $\sim 200 \mu\text{J}/\text{cm}^2$. As we can see from this figure there is an anomalous change of $\sim 4^\circ$ in the shear angle for this exposure level. No explanation can be offered for this anomalous increase in the shear angle, and this is because details about the shearing mechanism remain unclear. However, as this anomalous change does not appear for an interbeam angle of 40° and the values for the shear angle are different for 50° and 40° (see Figure

5), we can deduce that this anomalous effect has to be a function of the spatial frequency. Finally, in Figure 7 we have plotted the values obtained for the quotient t_e/t_c -using equation (4)- as a function of exposure. This parameter takes into account the differences between the effective thickness and the real thickness after processing.

All results presented in this section allow us to conclude that shear angles are a function of the recording material, processing, exposure, spatial frequency and slant angle.

4.- Spherical object wave studies

In more general devices such as lenses, the slant angle and the spatial frequency vary over the hologram surface, and consequently shear angles will also vary. In order to analyze the shear-type effects in holographic lenses (HL's), a HL was recorded through the interference of a spherical wave from a point source and a plane wave (Figure 8) as thick-phase holograms in Agfa 8E75 HD emulsion, using the 632.8 nm radiation of a He-Ne laser of 15 mW. The point source for the spherical wave was a pinhole measuring 25 μm in diameter. Spurious reflections were eliminated by placing an index matched absorbing layer against the glass side of the photographic plate. Polarization of the recording beams was perpendicular to the plane in Figure 8, and the usable diameter of the lens was 8 cm. The object wave was an on-axis spherical wave and the reference wave was a plane wave at an angle of -40° . The distance between the point source of the spherical wave and the centre of the plate was 32.5 cm. We chose one of the recording waves as a plane wave in order to simplify both recording and testing.

Using the approximation of the local grating¹⁵, over any small region of the HL, the interference pattern approximates a plane grating, and therefore we can define an object angle for each point on the surface of the HL. If we only analyze the plane in Figure 8, the corresponding object angles in air have values between -7° and 7° for $x = -4$ cm and $x = +4$ cm, respectively, and spatial frequencies of the HL on the X axis vary from 823 lines/mm (for $x = -4$ cm) to 1208 lines/mm (for $x = +4$ cm). Values of the object beam angle, θ_0 , spatial frequency, f , and slant angle, ϕ , for local gratings situated at each x point considered are given in Table IV.

The exposure level used was $200 \mu\text{J}/\text{cm}^2$ at the centre of the lens and $150 \mu\text{J}/\text{cm}^2$ at the borders, with a beam ratio of ~ 1 . The exposed plate was developed in AAC developer. The developed plate was then rinsed briefly and bleached without a fixation step with an R-9 reversal bleach. As the thickness and average refractive index of the holographic recording material change and shear-type effects appear when this chemical processing is used, the reconstruction geometry of the lens corresponding to maximum diffraction efficiency will not coincide with the construction geometry even though recording and readout wavelengths are equal. In order to comply with Bragg's law, we have to change the read-out geometry in relation to the recording geometry.

Once the lens was processed, the next step was to find the diffraction efficiency as a function of the reconstruction angle in order to show the presence of shear-type effects. The reconstruction of the HL was carried out according to the geometry in Figure 9. Since at each point of the HL the exposure value, the spatial frequency and the slant angle of the interference fringes were different, the diffraction efficiency was different as well. Due to this we determined the local efficiency for a general reconstruction angle, θ_C , by using a narrow probe beam of light, which was scanned across a lens diameter. We only obtained the angular response on the X axis points of the lens and we chose to use the points that go from -4 cm to $+4 \text{ cm}$ as values of x at 1 cm intervals. We also identified the value of the reconstruction angle θ_C that produces maximum diffraction efficiency in each case. This allowed us to obtain the deviation of the Bragg angle, $\Delta\theta_B = \theta_C - \theta_R$. The reconstruction beam was polarized perpendicular to the plane of Figure 8, like the recording beams, and the readout wavelength was 632.8 nm . The measurements of the angles were taken by using a rotation stage with a precision of 0.02° , also used in recording. Measurements of the local efficiency were obtained at 1° increments around the angle of the reference beam (-40°) between -30° and -50° .

We obtained the values of the shear angles δ using equations (14) and (19), and we calculated parameter t_e/t_C using the equation (4). In Figure 10 we show the results obtained. As we can see from this figure, since at each point of the lens the exposure values, the spatial frequency and the slant angle of the interference fringes are different, the shear angles and t_e/t_C

parameter are different as well. On the other hand, the values for δ obtained are similar to those calculated for the same exposure and for an interbeam angle of 40° . In particular, for $x = 0$ cm ($\theta_O = 0^\circ$, $\theta_R = -40^\circ$, $\phi = 11.54^\circ$ and $E = 200 \mu\text{J}/\text{cm}^2$) we obtained $\delta \approx 1.4^\circ$, while for the holographic gratings with the same geometrical parameters we obtained $\delta \approx 1.0^\circ$ (see Figure 5). This change in the reconstruction geometry of the HL with respect to the recording geometry gives rise to the appearance of aberrations. We can say that these aberrations have been induced by index and thickness changes as well as shear-type effects¹⁰ and these aberrations are equivalent to those that appear when we must vary the read-out geometry of the lens due to changes in the read-out wavelength in order to fulfill Bragg's law during the reconstruction stage¹⁶.

5.- Conclusion

We performed an experimental study of transmission holograms using Agfa 8E75 HD photographic emulsion and an R-9 reversal bleach without a fixation step. The index and thickness changes and the shearing of recording material due to processing were investigated, and the shear angles calculated from the deviation of the Bragg angle measurements are provided. The shear angle was obtained by using the theoretical equations from EHGM and we found that the deviation of the Bragg angle is a function of the shear angle, the index variations and the thickness change. Another important conclusion is that shear angles are a function not only of exposure (like index and thickness changes) but also of the slant angle and spatial frequency. Finally, the results analyzed in this paper should be particularly useful for holographic lenses design, in which recording material plays an essential role.

Acknowledgments

The authors would like to thank the reviewer of this paper for his very useful suggestions and for his comments, which significantly improved the original manuscript.

REFERENCES

- 1 **Swift, D. W.** "The application of holographic optical elements to head-up displays", *Proc. Inst. Radio. Electron. Eng. Austr.* **76**, (1987) 93-97
- 2 **Kostuk, R. K., Goodman, J. W., Hesselink, L.** "Design consideration for holographic optical interconnects", *Appl. Opt.* **26**, (1987) 3947-3957
- 3 **Vilkomerson, D. H. R., Bostwick, D.** "Some effects of emulsion shrinkage on a hologram's image space", *Appl. Opt.* **6**, (1967) 1270-1272
- 4 **McMahon, D. H., Caulfield, H. J.** "A technique for producing wideangle holographic displays", *Appl. Opt.* **9**, (1970) 91-96
- 5 **Beléndez, A., Pascual, I., Fimia, A.** "Model for analyzing the effects of processing on recording material in thick holograms", *J. Opt. Soc. Am. A* **9**, (1992) 1214-1223
- 6 **Beléndez, A., Pascual, I., Fimia, A.** "Efficiency of thick phase holograms in the presence of shear-type effects due to processing", *J. Modern Opt.* **39**, (1992) 889-899
- 7 **Rhee, U., Caulfield, H. J., Shamir, J., Vikram, C. S., Mirsalehi, M. M.** "Characteristics of the Du Pont photopolymer for angularly multiplexed page-oriented holographic memories", *Opt. Eng.* **32**, (1993) 1839-1847
- 8 **Mikhailov, I. A.** "A geometrical analysis of thick holograms", *Opt. Spectrosc.* **58**, (1985) 374-376
- 9 **Beléndez, A., Pascual, I., Fimia, A.** "Influences of recording materials in HOE", *Proc. SPIE* **1136**, (1989) 58-65

- 10 **Beléndez, A., Pascual, I., Fimia, A.** "Optimization of reconstruction geometry for maximum diffraction efficiency in HOE: The influence of recording material", *Proc. SPIE* **1574**, (1991) 77-83
- 11 **Kostuk, R. K.** "Factorial optimization of bleach constituents for silver halide holograms", *Appl. Opt.* **30**, (1991) 1611-1616
- 12 **Crespo, J., Fimia, A., Quintana, J. A.** "Fixation-free methods in bleached reflection holography", *Appl. Opt.* **25**, (1986) 1642-1645
- 13 **Syms, R. R. A., Solymer, L.** "Planar volume phase holograms formed in bleached photographic emulsions", *Appl. Opt.* **22**, (1983) 1479-1496
- 14 **Belenguer, T., de Miguel, L., Tornos, J., Quintanilla, M.** "Measuring the thickness and refractive index of thin layers: The influence of humidity on photographic emulsions", *Opt. Pura Apl.* **23**, (1990) 161-171
- 15 **Olson, D. W.** "The elementary plane-wave model for hologram ray-tracing", *Am. J. Phys.* **57**, (1989) 445-455
- 16 **Amitai, Y., Friesem, A. A., Weiss, V.** "Designing holographic lenses with different recording and readout wavelengths", *J. Opt. Soc. Am. A* **7**, (1990) 80-86

FIGURE CAPTIONS

- Figure 1.- Diagram showing the geometry of the holographic grating before and after processing as well as the different parameters used in this study. R, O and C are the reference, object and reconstruction beams, respectively.
- Figure 2.- Schematic diagram to obtain the relationship between the grating parameters before and after processing.
- Figure 3.- Experimental measurements of the $(\Delta n_R/n_R) - (\Delta t_R/t_R)$ parameter as a function of exposure. The solid curve shows the adjustment of the experimental data by a cubic polynomial curve using a least squares method.
- Figure 4.- The angular deviation between the Bragg angle and the reference angle, $\Delta\theta_B$, as a function of exposure for different slant angles and for interbeam angles of (a) 50° and (b) 40° .
- Figure 5.- The shear angle as a function of exposure for different slant angles and for interbeam angles of (a) 50° and (b) 40° .
- Figure 6.- The shear angle δ as a function of exposure for an interbeam angle of 50° and for a slant angle of 13.92° . The dotted line links the experimental points and the solid line corresponds to the theoretical adjustment of the experimental data without taking into account the anomalous point for an exposure of $\sim 200 \mu\text{J}/\text{cm}^2$.
- Figure 7.- The t_e/t_C parameter as a function of slant angle for different exposures and for interbeam angles of (a) 50° and (b) 40° .

Figure 8.- The recording geometry of the holographic lens analyzed. The reference beam is collimated and the object beam is divergent.

Figure 9.- The experimental reconstruction geometry used for local testing of HL's. The reconstruction is made by using a narrow probe beam of light, which was scanned across the lens diameter in the X axis direction.

Figure 10.- The angular deviation between the Bragg angle and the reference angle, $\Delta\theta_B$, the shear angles, δ , and the t_e/t_C parameter, as a function of the points on the X axis of the lens aperture.

TABLES

Table I.- Processing schedule.

Table II.- Developer and bleach bath formulae.

Table III.- Recording geometries and the corresponding values of slant angles of interference fringes and spatial frequencies for (a) 50° and (b) 40° interbeam angles.

Table IV.- Geometrical characteristics of the holographic lens analyzed experimentally. The angle of the reference beam is $\theta_R = -40^\circ$.

TABLE I

-
1. Develop for 4 min at 20°C
 2. Rinse in running water for 1 min at 20°C
 3. Bleach for 1 min after the plate has cleared at 50°C
 4. Wash in running water for 5 min at 20°C
 5. Dry (20°C and 60% RH)
-

TABLE II

AAC DEVELOPER

1-Ascorbic acid	18 g
Sodium carbonate	60 g
Distilled water to make	1 litre

REVERSAL R-9 BLEACH BATH

Potassium dichromate	2 g
Sulphuric acid, conc.	10 ml
Distilled water to make	1 litre

TABLE III

(a) $|\theta_R| + |\theta_0| = 50^\circ$

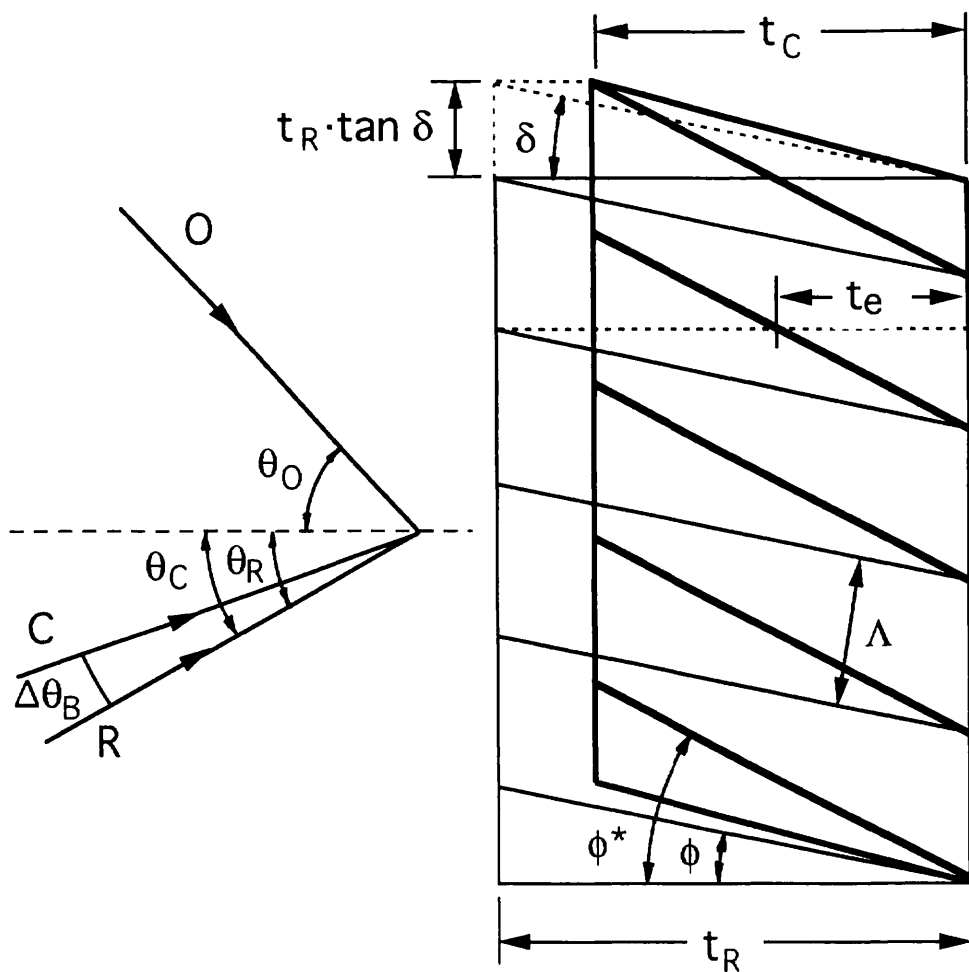
θ_R	θ_0	ϕ	f (lines/mm)
0°	-50°	13.92°	1210
5°	-45°	11.25°	1255
10°	-40°	8.50°	1290
15°	-35°	5.70°	1315
20°	-30°	2.86°	1330

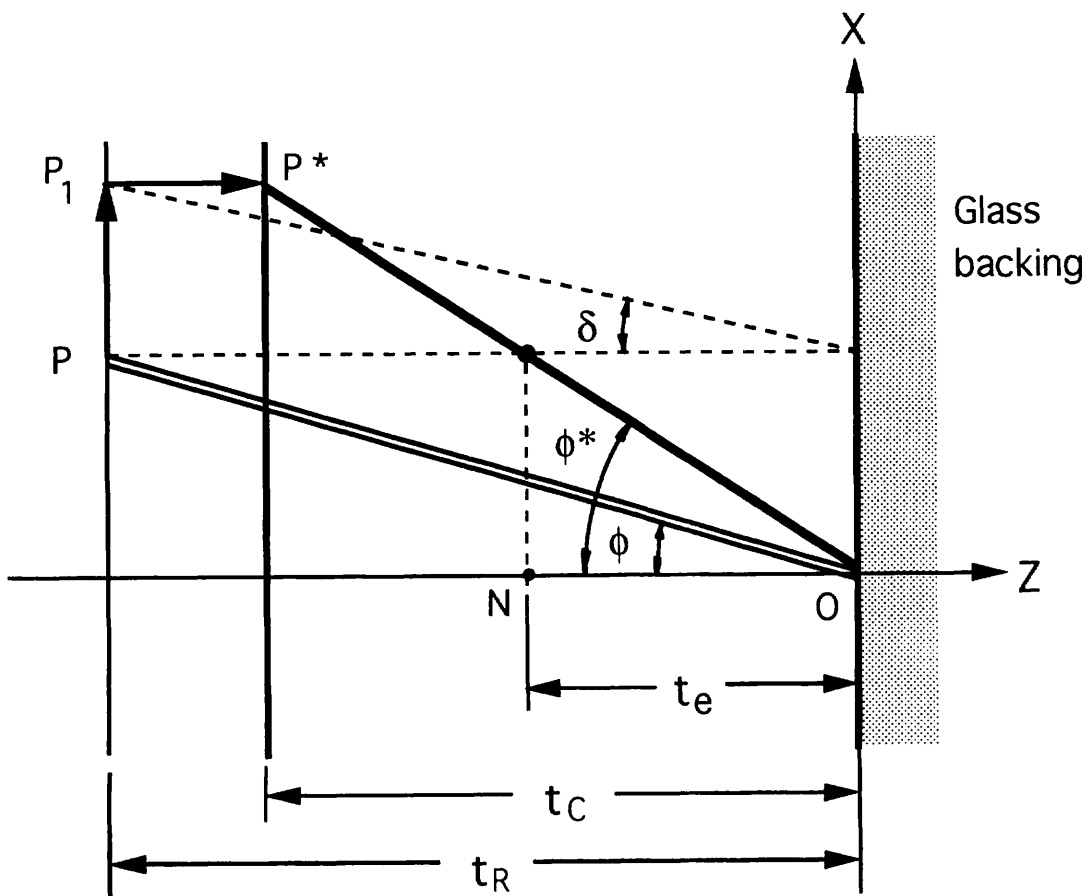
(b) $|\theta_R| + |\theta_0| = 40^\circ$

θ_R	θ_0	ϕ	f (lines/mm)
0°	-40°	11.54°	1015
5°	-35°	8.71°	1044
10°	-30°	5.84°	1064
15°	-25°	2.93°	1077

TABLE IV

x (cm)	θ_0	f (lines/mm)	ϕ
+ 4	7.0°	1208	9.41°
+ 3	5.3°	1161	9.92°
+ 2	3.5°	1112	10.47°
+ 1	1.8°	1065	10.99°
0	0.0°	1015	11.54°
- 1	$- 1.8^\circ$	966	12.09°
- 2	$- 3.5^\circ$	919	12.60°
- 3	$- 5.3^\circ$	870	13.15°
- 4	$- 7.0^\circ$	823	13.67°





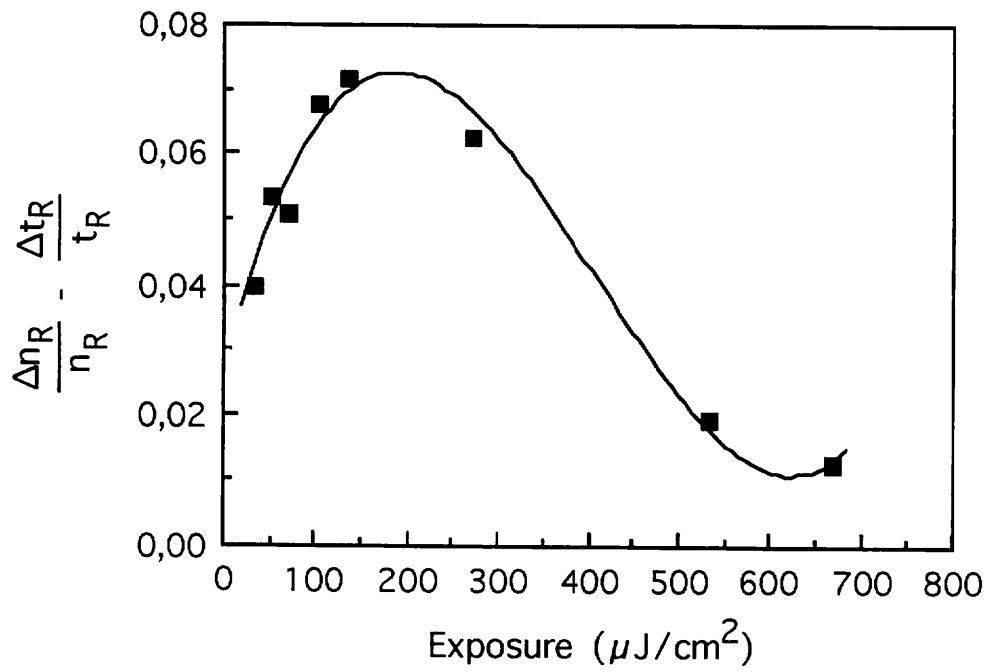
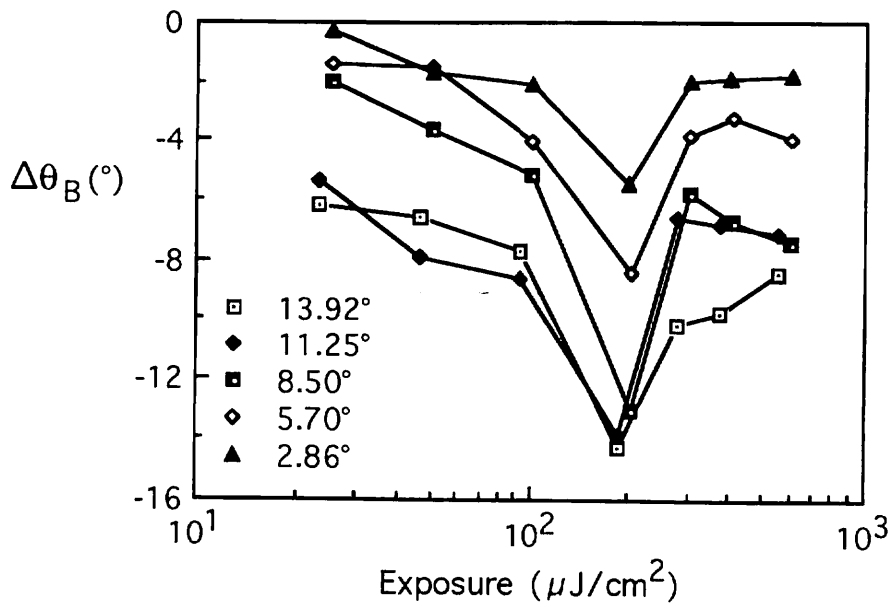


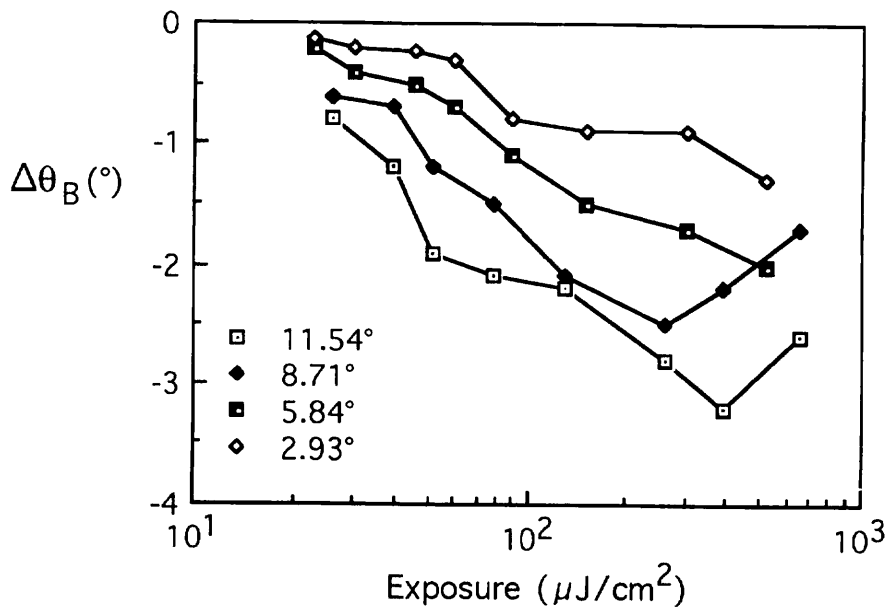
FIGURE 3

BELÉNDEZ, Augusto; CARRETERO, Luis; FIMIA, Antonio. "Experimental evaluation of shearing effects in volume holograms formed in bleached photographic emulsions". Optics & Laser Technology. Vol. 26, Issue 5 (1994). ISSN 0030-3992, pp. 341-349

A. Beléndez et al.

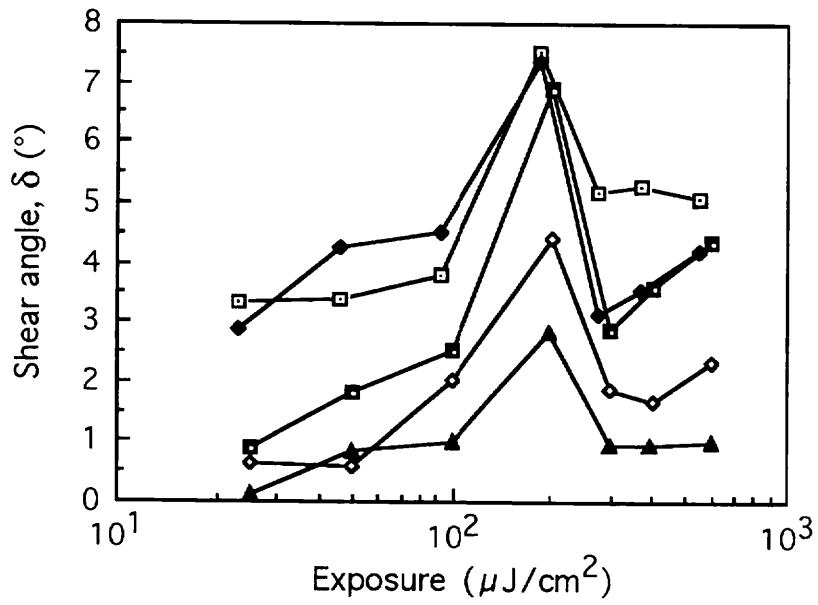


(a)

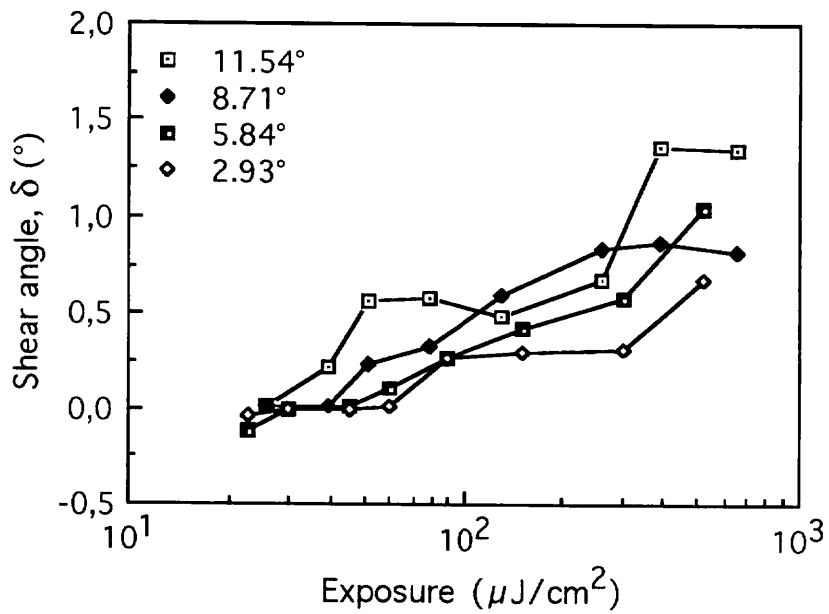


(b)

FIGURE 4



(a)



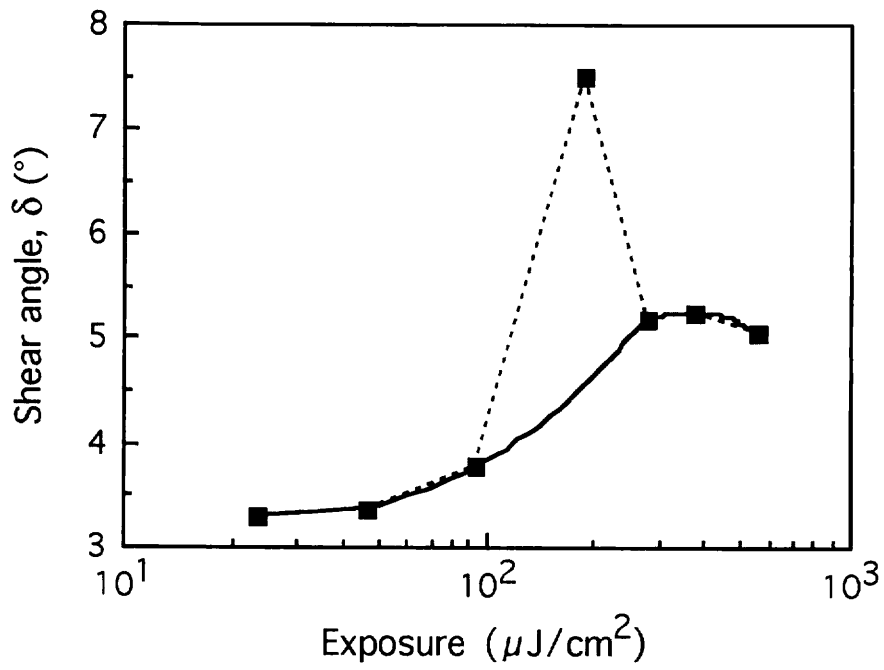
(b)

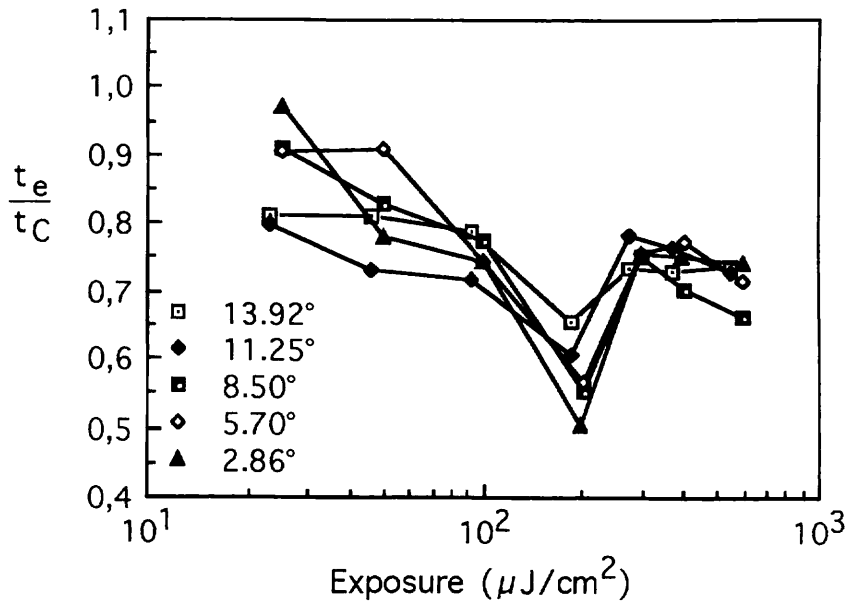
FIGURE 5

BELÉNDEZ, Augusto; CARRETERO, Luis; FIMIA, Antonio. "Experimental evaluation of shearing effects in volume holograms formed in bleached photographic emulsions". Optics & Laser Technology. Vol. 26, Issue 5 (1994). ISSN 0030-3992, pp. 341-349

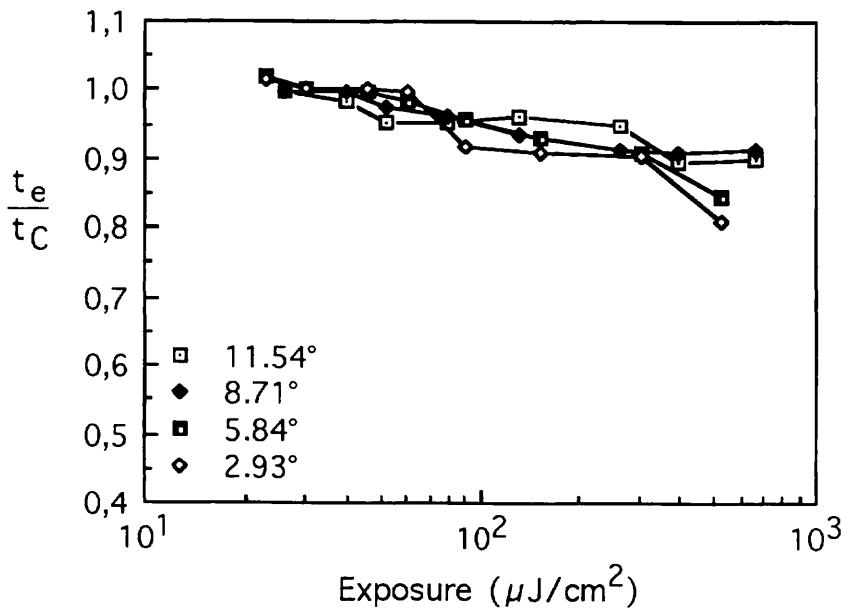
DOI: 10.1016/0030-3992(94)90121-X

A. Beléndez et al.

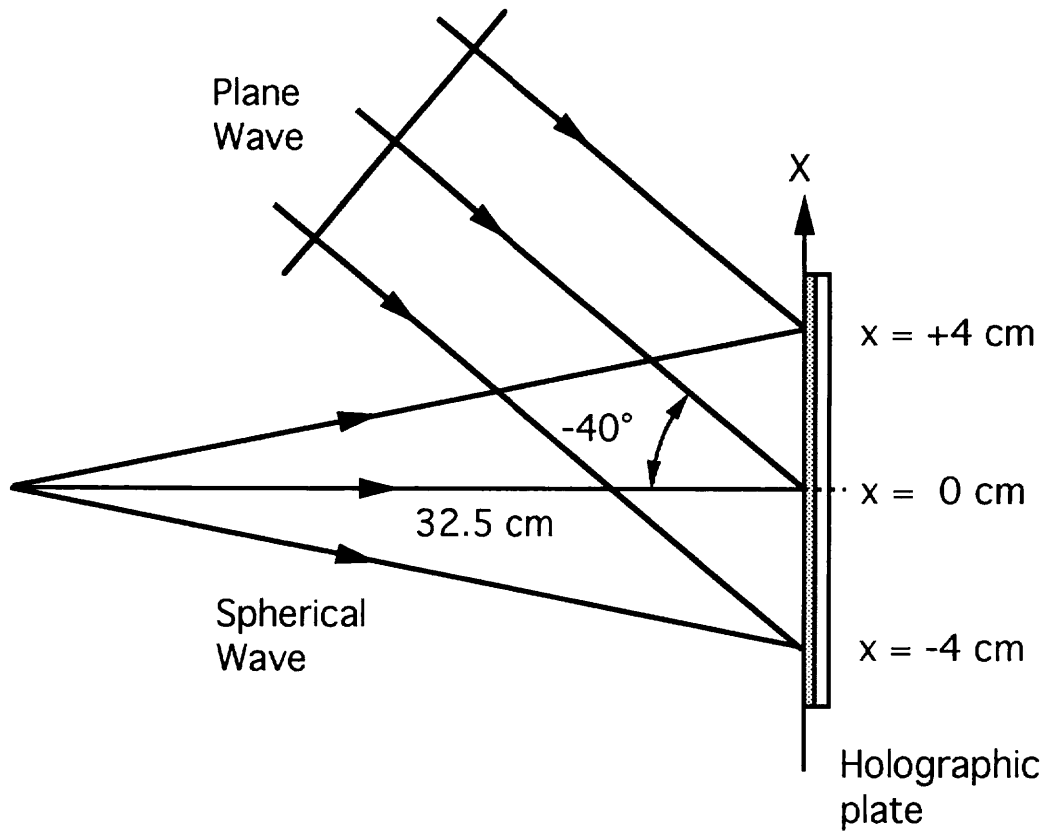




(a)



(b)



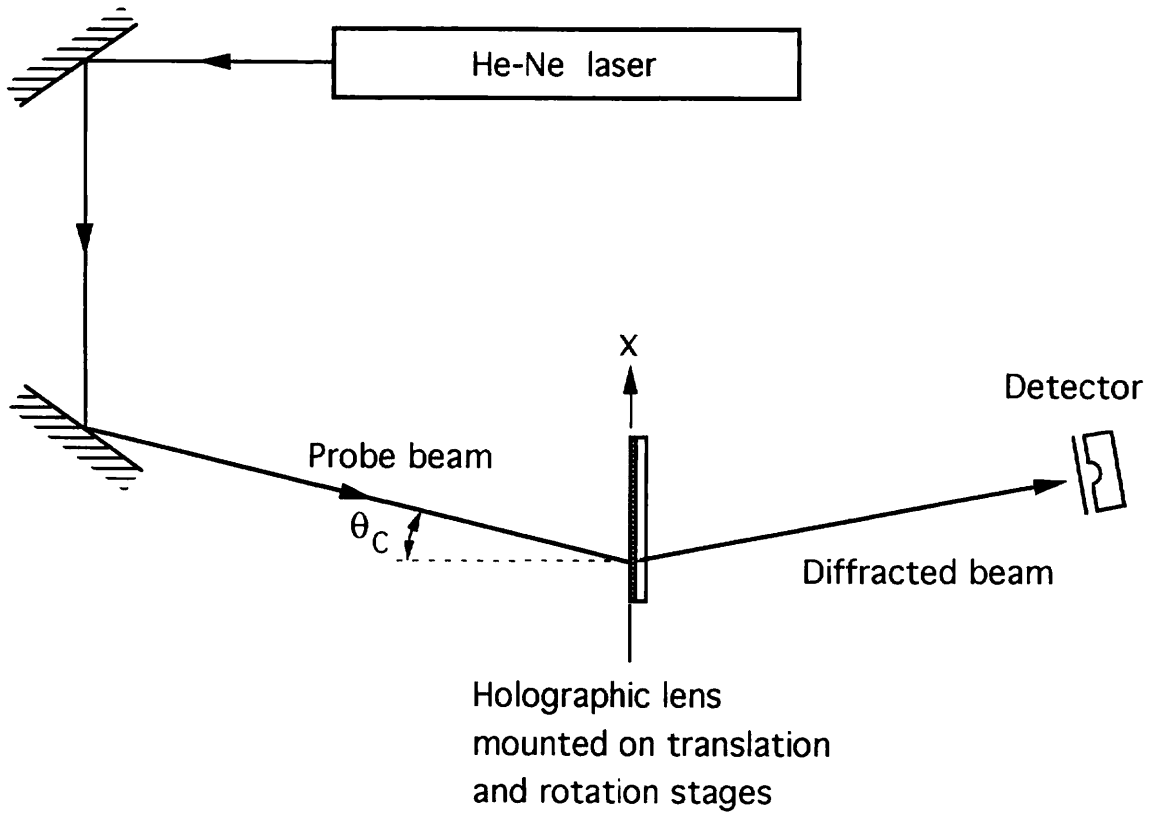


FIGURE 9
A. Beléndez et al.

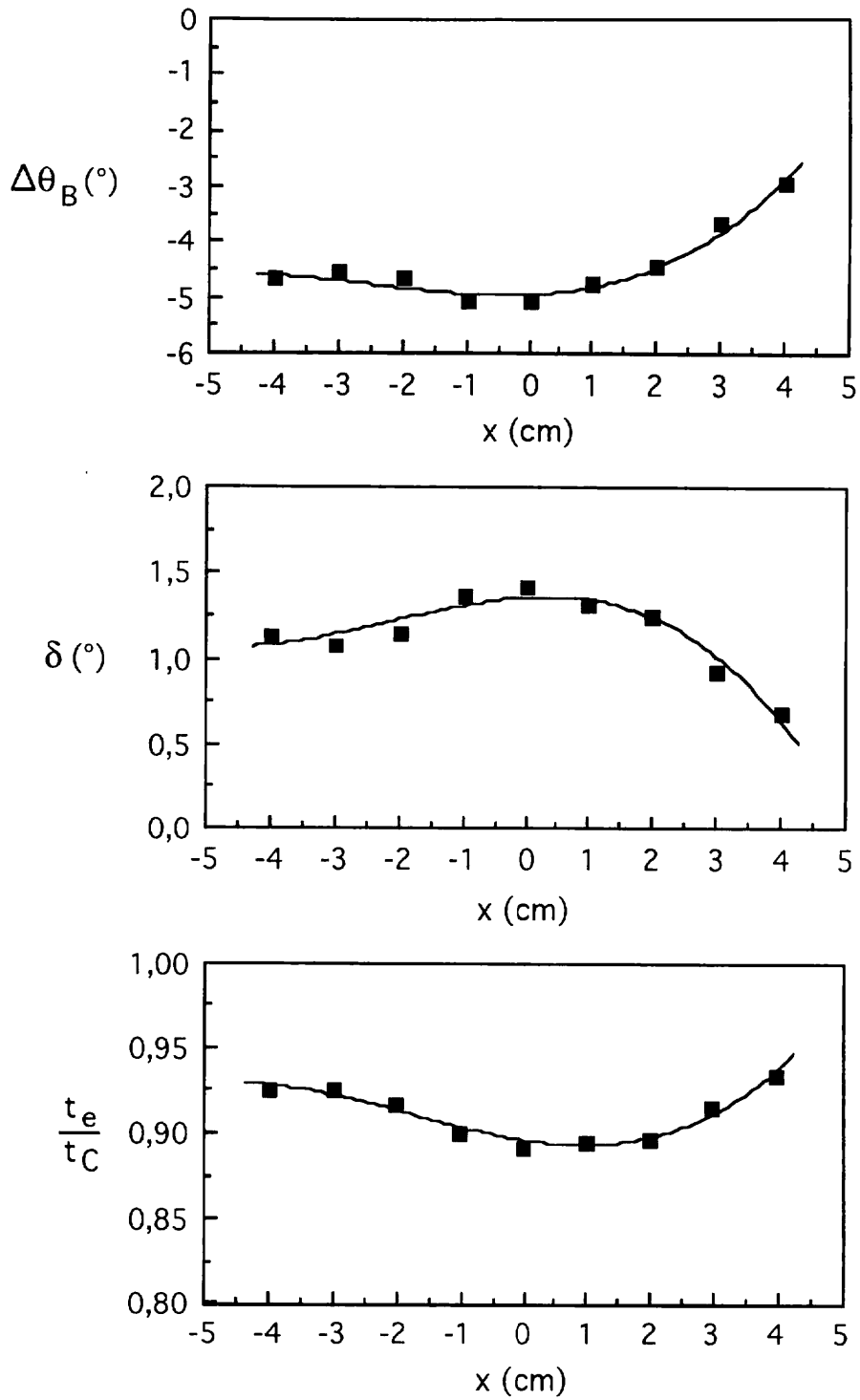


FIGURE 10
A. Beléndez et al.